

EXPERIMENTAL INVESTIGATION OF PULSED LASER HEATING OF THERMIONIC CATHODES IN RF GUNS*

N. Sereno, M. Borland, K. Harkay, Y. Li, R. Lindberg, S. Pasky[†], ANL, Argonne, IL 60439, USA

Abstract

One proposed injector for the X-ray Free Electron Laser Oscillator [1] uses a 100 MHz thermionic rf gun to deliver very small emittances at a 1 MHz rate [2]. Since the required beam rate is only 1 MHz, 99% of the beam must be dumped. In addition, back-bombardment of the cathode is a significant concern. To address these issues, we propose [3] using a laser to quickly heat the surface of a cathode in order to achieve gated thermionic emission in an rf gun. We have investigated this concept experimentally using an existing S-band rf gun with a thermionic cathode. Our experiments confirm that thermal gating is possible and that it shows some agreement with predictions. Operational issues and possible cathode damage are discussed.

EXPERIMENTAL SETUP

The experiments described here were performed in the APS injector test stand (ITS). Figure 1 shows the ITS layout, where all distances are measured relative to the rf gun exit. The beam may be directed either straight to the stripline and Faraday Cup (FC), or bent by the dipole to a flag for energy measurement. The figure also shows a mirror that allows transporting a laser beam to the center of the gun cathode. The primary diagnostics for the experiment are the FC and integrating current transformer (ICT). The goal of the experiment is to see how short a beam pulse can be gated from the cathode using the near-infrared laser ($\lambda = 1\mu\text{m}$) for various gun, rf, and cathode heater parameters. Measurements of the beam at the ICT and FC are read out on a scope for immediate viewing and offline data analysis.

FIRST MEASUREMENTS OF THERMIONIC EMISSION DUE TO THE LASER

In these experiments, the rf gun used was a spare gun that is normally not used for operations. In all the experiments, the rf gun forward power was set to 3.6 MW, resulting in a beam kinetic energy of 2.8 MeV. This power corresponds to $\approx 50\text{MV/m}$ gradient at the cathode. The rf repetition rate was 6 Hz with a pulse length of $1\mu\text{s}$. The gun cathode used was a tungsten dispenser cathode with barium oxide used to lower the work function. Figure 2 shows the current pulse measured on the FC, where we see the long current pulse

due to the $\approx 1\mu\text{s}$ rf pulse along with a very short spike near the peak of the rf pulse. This spike is due to thermionic emission triggered by the 5 ns FWHM infrared laser pulse. The laser timing was adjusted relative to the rf pulse so that the laser pulse arrived at the cathode at the peak rf gun field. The peak gun field level occurs just before the long ($1\mu\text{s}$) current pulse starts to drop as shown in the plot.

Next, the gun cathode heater power was lowered to 11.2 W until no thermionic emission was observed without the laser. The total charge in the spike was then measured using the ICT, allowing us to calibrate the FC signal. We could easily obtain 150 pC total charge and 20 mA peak current on the FC using an average laser power of 22.5 mW (0.6 MW peak laser power for 6 Hz rep rate and $\sigma = 2.5\text{ ns}$ or 3.75 mJ/pulse). This corresponds to an average laser energy density of 260 mJ/cm² on the cathode. This is about 3 times the total charge required by the XFEL-O injector gun. Ultimately, this experiment would need to be repeated using a CeB₆ cathode under realistic conditions (e.g., 1 MHz rate) to determine the applicability of laser gating to the XFEL-O.

FARADAY CUP CURRENT MEASUREMENTS AND FITS

We developed a simple theory [3] based on the Richardson-Dushman equation and the 1-dimensional diffusion equation to describe the laser gating process. The theory yields an expression for the current as a function of cathode, laser, and rf gun parameters according to,

$$I(t) = a_0 T^2(t) e^{-\phi_{WS}/(kT(t))} \quad (1)$$

$$a_0 = \pi R^2 A_0 e^{-\alpha/k} \quad (2)$$

$$T(t) = \tau_0 + P_{av} a_1 G(t) \quad (3)$$

$$a_1 = \frac{\epsilon}{\pi^2 r \sigma \rho C_p R^2 \sqrt{2\kappa}} \quad (4)$$

$$\phi_{WS} = \phi_W - \sqrt{\frac{e^3 E_s}{4\pi\epsilon_0}} \quad (5)$$

Where ϵ , ρ , C_p , $\kappa = \frac{K}{\rho C_p}$, A_0 , k , K , α and ϕ_W are respectively the emissivity, mass density, specific heat capacity, thermal diffusivity, Richardson constant, Boltzmann's constant, thermal conductivity, linear work function temperature coefficient, and work function of the dispenser cathode; P_{av} , r , R , σ , and Δt (not shown in the equations) are the average laser power, repetition rate, laser spot radius on the cathode, laser temporal rms width, and laser time offset, which specifies when the laser reaches peak power. $E_s = 50\text{ MV/m}$ is the rf gun accelerating gradient at the

* Work supported by the U.S. Department of Energy, Office of Science, Office of Basic Energy Sciences, under Contract No. DE-AC02-06CH11357.

[†] sereno@aps.anl.gov

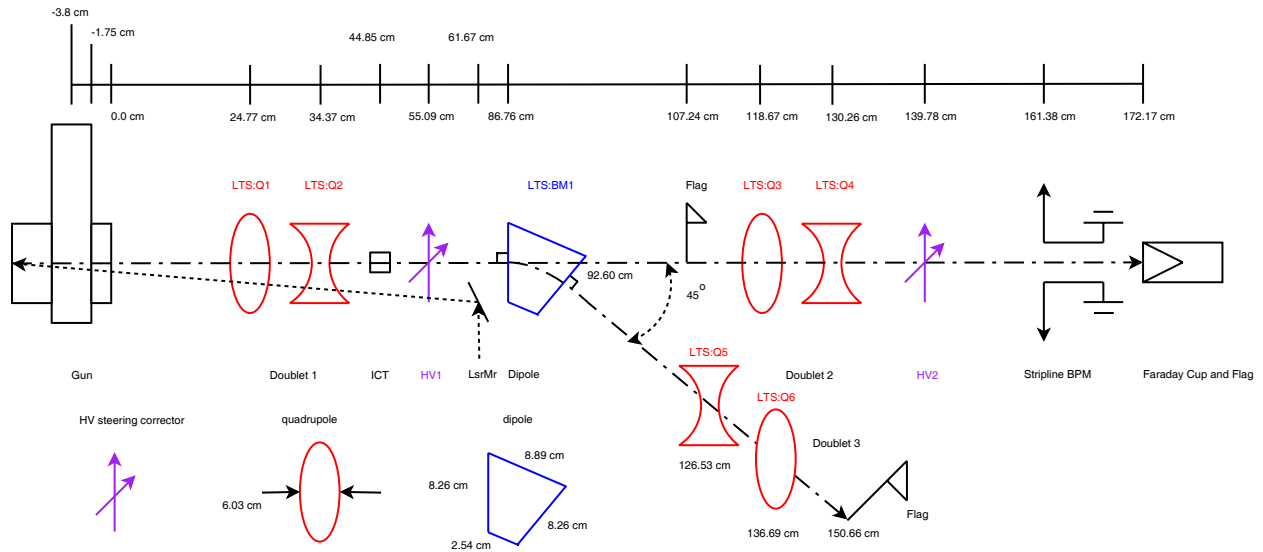


Figure 1: ITS layout showing magnets and diagnostics components. See text for discussion.

cathode. The function $G(t)$ is the Green's function integral, which depends on the laser pulse profile and gives the time dependence of the cathode current emission. When evaluating the above constants, we use the bulk material properties of tungsten, except for the Richardson constant where we use its corrected value $A_0 = 1.5 \text{ A/cm}^2\text{K}^2$ and the lowered work function $\phi_W = 1.67 \text{ eV}$ which is reduced (from that of pure tungsten) by the barium diffused through the tungsten cathode [4, 5]. The laser spot size parameter was estimated to be $R = 0.5 \text{ mm}$ for our $\sigma = 2.5 \text{ ns}$ laser which is capable of 200 mW average power at a 6 Hz rate (33.3 mJ/pulse). We use Eq. 1 as the fitting function for two sets of measurements: in the first set, we fit the measured peak FC current as a function of average laser power. In the second set, we fit the temporal FC pulse shape. For the first set of measurements, we are able to measure the product $a_1 G(t_{peak})$, where $t = t_{peak}$ is the location of the maximum of the Green's function integral. For the second set, we use fitting to determine σ , Δt , and $a_1 P_{av}$. In both cases we used $a_0 = 0.36 \text{ mA/K}^2$ and $\phi_{eff} = 1.4 \text{ eV}$ (using $E_s = 50 \text{ MV/m}$), based on known values.

Peak FC Current vs Average Laser Power

We acquired 30 samples of FC peak current and average laser power values for various average power settings of the laser. We then computed the average and standard deviation of the FC from the 30 waveforms. Figure 3 shows the result of fitting the peak current vs laser power using Eq. 1 and sddsgenericfit [6], which can fit arbitrary functions including error bars. Each curve represents a different gun heater power level or, equivalently, offset temperature τ_0 . Using the parameters for the cathode, laser and rf gun from the previous section, we calculate $a_1 G(t_{peak}) = 65.6 \text{ K/mW}$ for a peak Green's function integral value of $G(t_{peak}) = 1.28 \times 10^{-4} \text{ s}^{1/2}$.

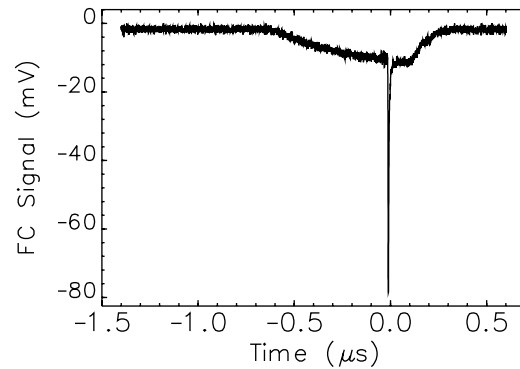


Figure 2: RF gun thermionic current pulse ($\approx 1 \mu\text{s}$) along with the short $\sigma \approx 2.5 \text{ ns}$ current pulse due to the infrared laser, as seen on the Faraday cup.

The fits, summarized in Table 1, turned out to be quite good and generally show increasing offset temperature τ_0 vs heater power. The notable exception is the 4.65 Watt heater power case which may be due to not allowing enough time for the cathode and gun assembly to reach thermal equilibrium. The average value of a_1 is 26.5 K/mW , about a factor of 2.5 lower than the expected value. This implies a temperature rise in the part of the cathode illuminated by the laser of 530 K for an average laser power of 20 mW . Possible explanations for the discrepancy are the temperature dependence of the bulk material properties of tungsten (we used room temperature values in estimating a_1), errors in the assumed emissivity, and errors in the assumed laser spot size.

Time Domain Pulse Shape Fitting

In this analysis we fit the temporal pulse shape of the current spike, using the the material, laser, and gun parameters

Table 1: Fit Parameters for each Heater Power Shown in Fig. 3, Taking $a_0 = 0.36 \text{ mA}/\text{K}^2$.

Heater Power (W)	$a_1 G(t_{peak})$ (K/mW)	τ_0 (K)
4.65	23.9	647
7.31	28.1	601
9.71	29.2	778
9.75	23.5	839
10.3	27.7	847

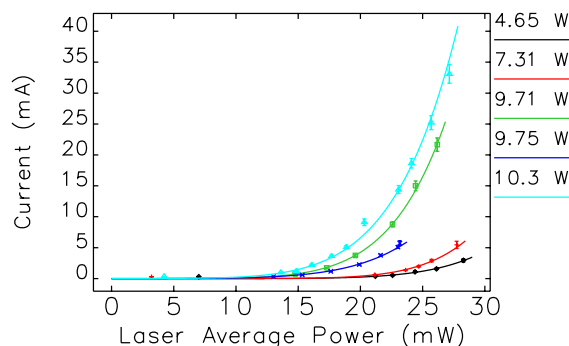


Figure 3: FC peak current vs laser power and fit for various heater powers.

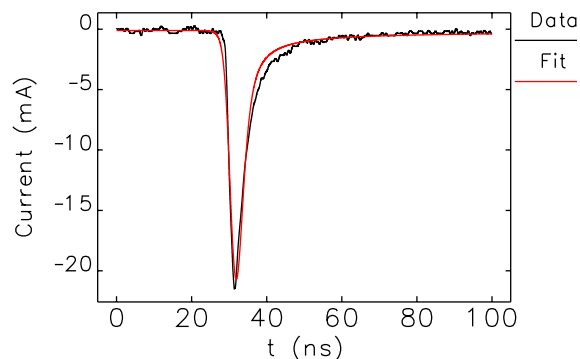
listed above. We again use `sddsgenericfit`, this time varying the laser rms width parameter $\sigma \approx 2.5 \text{ ns}$ and offset time Δt . Figure 4 shows the result for the fit to a pulse of 21 mA amplitude. The fit reproduces the peak amplitude to within about 3.5%, with a shape that matches the measured shape, but has a faster fall time. This is likely due to bandwidth of the Faraday cup. The best-fit laser parameters σ and Δt are close to the expected laser pulse width of 2.5 ns and the FC peak amplitude.

We fit eight pulses measured at the FC ranging from 5 to 21 mA peak amplitude, three of which were at measured at a heater power of 11.3 W and five of which were at 9.3 W. We used $a_0 = 0.36 \text{ mA}/\text{K}^2$ calculated in the previous section for all fits. About 25% variation was seen in the $a_1 P_{av}$ with no clear relationship observed to heater power. We expected $a_1 P_{av}$ to fall in the range $0.5 - 2.6 \times 10^7 \frac{\text{K}}{\sqrt{s}}$ for average laser powers in the 10 to 50 mW range used in these experiments. Our fit values averaged $0.33 \times 10^7 \frac{\text{K}}{\sqrt{s}}$ which yields a 422 K temperature rise when using $G(t_{peak})$ from the previous section. The range of values of τ_0 was 980 to 1070 K, with no clear correlation with heater power. Hence, although we were able to reproduce the functional form of the current pulse, we were not able to extract detailed values. Very likely this is owing to a considerable amount of degeneracy among the parameters.

These experiments could be improved in a number of ways. First, we can measure τ_0 off-line using a pyrometer. By calibrating the filament resistance vs the pyrometric temperature, we should have a reliable proxy for a direct temperature measurement. Second, monitoring of the filament resistance should be performed to verify that the cathode temperature has stabilized after changes. Third, we can

04 Extreme Beams, Sources and Other Technologies

4E Sources: Guns, Photo-Injectors, Charge Breeders


 Figure 4: Best fit to the FC current pulse shape for the maximum peak current, giving $\sigma = 2.48 \text{ ns}$, $\Delta t = 1.43 \text{ ns}$, and $a_1 P_{av} = 3.6 \times 10^6 \frac{\text{K}}{\sqrt{s}}$.

check the values of a_0 and ϕ_{WS} using purely thermionic emission, although this will be involved due to difficultly determining the gradient at the cathode. Finally, we've recently purchased a high-bandwidth Faraday cup, which will allow better resolution of the detailed pulse shape.

CONCLUSION

Experiments have been performed in which a nanosecond laser pulse was used to flash heat a thermionic cathode over the emission threshold. Measurements were made of the peak current and the current profile. These show reasonable agreement with expectations based on the Richardson-Dushman equation and a one-dimensional model of temperature rise from the diffusion equation. In particular, nanosecond beam pulses were created with 150 pC charge. Some of the observed discrepancies are likely due to bandwidth limitations of the Faraday cup. Although the pulse shape agreed reasonably well with the simulations, we were not able to extract detailed values of parameters in a satisfying way. To ascertain applicability of laser gating of a thermionic cathode for application to the XFEL-O injector, these experiments need to use a CeB_6 cathode and realistic repetition rates of around 1 MHz.

ACKNOWLEDGMENTS

We thank the APS Diagnostics Group, Rf Group, and Mechanical Operation and Maintenance Group for setting up equipment that made these experiments possible.

REFERENCES

- [1] K. J. Kim *et al.*, Phys. Rev. Lett. 100, 244802 (2008).
- [2] P. N. Ostroumov *et al.*, Proc. LINAC08, 676-678 (2008).
- [3] M. Borland *et al.*, these proceedings.
- [4] B. Wolf, *Handbook of Ion Sources*, CRC Press, 27 (1995).
- [5] C. J. Smithells, *Metals Reference Book*, Vol III, Butterworths, London, 737 (1967).
- [6] M. Borland, Proc. PAC95, 2184 (1996).